

**Black-hole binary simulations: The mass ratio 10:1**José A. González,<sup>1,2</sup> Ulrich Sperhake,<sup>1,3,\*</sup> and Bernd Brügmann<sup>1</sup><sup>1</sup>*Theoretisch-Physikalisches Institut, Friedrich-Schiller-Universität, 07743 Jena, Germany*<sup>2</sup>*Instituto de Física y Matemáticas, Universidad Michoacana de San Nicolás de Hidalgo, Morelia, Michoacán, Mexico*<sup>3</sup>*Theoretical Astrophysics 350-17, California Institute of Technology, Pasadena, California 91125, USA*

(Received 24 November 2008; published 5 June 2009)

We present the first numerical simulations of an initially nonspinning black-hole binary with mass ratio as large as 10:1 in full general relativity. The binary completes approximately three orbits prior to merger and radiates  $(0.415 \pm 0.017)\%$  of the total energy and  $(12.48 \pm 0.62)\%$  of the initial angular momentum in the form of gravitational waves. The single black hole resulting from the merger acquires a kick of  $(66.7 \pm 3.3)$  km/s relative to the original center of mass frame. The resulting gravitational waveforms are used to validate existing formulas for the recoil, final spin, and radiated energy over a wider range of the symmetric mass ratio parameter  $\eta = M_1 M_2 / (M_1 + M_2)^2$  than previously possible. The contributions of  $\ell > 2$  multipoles are found to visibly influence the gravitational wave signal obtained at fixed inclination angles.

DOI: [10.1103/PhysRevD.79.124006](https://doi.org/10.1103/PhysRevD.79.124006)

PACS numbers: 04.25.D-, 04.25.dg, 04.30.Db

**I. INTRODUCTION**

Following the breakthroughs of 2005 [1–3], the numerical relativity community has constructed several independent codes [4–12] and proceeded at a breathtaking speed in generating new insights into the dynamics of inspiralling and coalescing black-hole binaries (BBH) and the resulting gravitational wave patterns [13]. For example, numerical relativity has provided vital information regarding the kick or recoil in astrophysical mergers [14–23], simulations of spin flip and precession phenomena [15,24], and the interpretation of gravitational waveforms to be observed in the future [25–30]. See also [31–35] for binary simulations involving neutron stars. This progress has come timely, as earthbound gravitational wave detectors LIGO, VIRGO, GEO600, and TAMA [36–39] are now collecting data at or near the design sensitivity. The combined use of theoretical predictions and sophisticated data analysis methods will be crucial in achieving the first direct detection of gravitational waves and thus opening a new window to the Universe.

The purpose of this work is to extend the range of mass ratios probed by numerical relativity to  $q \equiv M_1/M_2 = 10$ , corresponding to  $\eta \equiv q/(1+q)^2 = 0.0826$ . This mass ratio is of particular interest for a variety of reasons. First, studies of the supermassive black-hole formation history, starting with light seed black holes, predict a significant fraction of mergers in the range  $1 \leq q \leq 10$  and, depending on accretion details, the possibility of a peak near  $q = 5, \dots, 10$  [40]. Similarly, detailed statistical analysis of the mass distribution of supermassive galactic black holes predicts that most mergers will occur in the range  $3 \leq q \leq 30$  [41]. Finally, accurate numerical simulations with  $q = 10$  will facilitate unprecedented compari-

sons with approximative calculations based on post-Newtonian expansions (cf. [42–45] as well as [46] for a review) and extreme mass ratio (EMR) predictions based on perturbation theory and self-force calculations (see [47–53] and references therein). By considering, for example, an expansion in the mass ratio parameter, a naive estimate of the error in perturbative calculations would be of the order of  $1/q^2$  or 1% relative to background quantities, or 10% for quantities of first order in  $1/q$ . While such comparisons are beyond the scope of this paper, we will lay the foundation for future work by giving a detailed convergence analysis of the numerical results including estimates for the uncertainties.

We will also use our results to probe recently published formulas for calculating the final spin and recoil resulting from the coalescence of two black holes with given initial physical parameters. Spin measurements of black holes via direct astrophysical observations have so far provided information about several individual holes [54–60] but appear as yet to be insufficient for constructing reliable spin-distribution functions. The community has therefore pursued the alternative path of using theoretical predictions in the context of the growth history and accretion processes of the holes [61–67]. It is important for the modeling of the individual binary mergers in such simulations to have available mappings between the initial parameters of the binary and the final spin and recoil of the post-merger remnant. A better understanding of the distribution function of the black-hole recoil also generates a great deal of interest in its own right. In particular, there remain open questions as to how generically recoil velocities of thousands of km/s result from astrophysically realistic binary mergers. Such large recoil would not only result in intergalactic populations of black holes but would also affect the central structure of galaxies and put severe constraints on possible scenarios of the black-hole formation history

\*sperhake@tapir.caltech.edu

[68–74]. For recent discussions on direct observational signatures of recoiling black holes, see also [75–77].

Existing formulas predicting the kick and final spin as functions of the initial parameters of the binary are based on simulations using mass ratios  $1 \leq q \leq 4$  or  $0.25 \geq \eta \geq 0.16$  and, in the case of Baker *et al.* [78], using also  $q = 6$  or  $\eta = 0.122$  for the final spin. Our results clarify the validity of these formulas in the case of initially non-spinning holes. We further analyze the multipolar structure of the resulting gravitational waveforms and illustrate the significance of the higher order multipoles in the gravitational wave signal.

The paper is organized as follows. We describe in Sec. II the numerical simulations together with a calibration of their uncertainties. In Sec. III, we analyze the gravitational waveforms generated in the inspiral with regard to the total amount of energy, linear, and angular momentum radiated, and test the validity of existing fitting formulas for final spin and recoil. We further demonstrate that a significant fraction of the energy is radiated in higher order multipoles, which implies that gravitational wave signals differ significantly from the typical quadrupole shape presented in most of the numerical relativity literature. We conclude in Sec. IV and discuss possible future studies based on the data presented in this work.

## II. NUMERICAL SIMULATIONS

We have performed our simulations using the BAM code as described in [4,79]. In order to obtain sufficient accuracy for this demanding type of simulation, we use sixth order discretization for the spatial derivatives [80] and fourth order accurate integration in time. Initial data are provided by the spectral solver described in Ref. [81]. Gravitational waves are calculated in the form of the Newman-Penrose scalar  $\Psi_4$  according to the procedure described in Sec. III in [4] (but see [82] for an alternative method to extract  $\Psi_4$ ).

The model we are focusing on in this work represents a black-hole binary with initial parameters as given in Table I. We follow the convention of [83] and normalize initial parameters relative to the total black-hole mass  $M = M_1 + M_2$  and dimensional diagnostic quantities by their total initial values: the Arnowitt-Deser-Misner (ADM) mass  $M_{\text{ADM}}$  and the total initial angular momentum  $J_{\text{ini}}$ . The initial tangential linear momentum  $P$  has been calculated from Eq. (65) of [4] which gives a third order post-

Newtonian estimate for the momentum of a quasicircular configuration. We calculate the number of orbits completed by this configuration from the waveform as described in Sec. III C of [83] and obtain about three orbits and six wave cycles.

The mass ratio  $q = 10$  does not require any changes in the construction of initial data. However, let us point out one important issue that affects the puncture evolution method. We use the “000” gauge advection choice; that is, we evolve the shift according to  $\partial_0 \beta^i = \frac{3}{4} B^i$  and  $\partial_0 B^i = \partial_0 \tilde{\Gamma}^i - \eta_s B^i$  with  $\partial_0 = \partial_t - \beta^i \partial_i$ . In second order form the shift condition is

$$\partial_0^2 \beta^i = \frac{3}{4} \partial_0 \tilde{\Gamma}^i - \eta_s \partial_0 \beta^i, \quad (1)$$

from which it is immediate that the physical dimension of the shift damping parameter  $\eta_s$  is

$$[\eta_s] = 1/M. \quad (2)$$

(We have added the label “s” to distinguish  $\eta_s$  from the mass ratio  $\eta$  used elsewhere.) The parameter  $\eta_s$  was introduced to control the dynamics of the shift vector [84,85]; in particular, it influences the degree of slice stretching that develops near the black holes during dynamic gauge evolution, but  $\eta_s$  also affects the drift of coordinates near the outer boundary. Only certain values of  $\eta_s$  lead to stable evolutions. This also applies to evolutions in the moving puncture framework; see e.g. [4] for a discussion of some of the  $\eta_s$  dependence found in our evolutions, and [86] for related discussions.

The issue that arises for  $q = 10$  is that  $\eta_s$  is chosen to be a global constant, say  $\eta_s = 2.0/M$ , but the effect of  $\eta_s$  on the slice stretching near the black holes is different if the black-hole masses are different. Assuming that  $\eta_s = 2.0/M$  is a good choice near the black holes for equal mass,  $M_1 = M_2 \approx M/2$ , then increasing  $M_1$  by a factor of 5 means that  $\eta_s$  has to be replaced by  $\eta_s/5$  to obtain the same amount of slice stretching. Similarly, if  $M_2$  is reduced, then  $\eta_s$  should be correspondingly enlarged.

For these reasons the standard choice of  $\eta_s = 2.0/M$  made in [4] did not work for  $q = 10$  evolutions; the effective  $\eta_s$  near the black holes did not lead to stable and accurate evolutions. A telltale sign for  $\eta_s$  being too large is if the orbits drift outwards rather than spiral inwards, which is accompanied by a loss of convergence with time. Numerical experiments revealed that  $\eta_s$  can be

TABLE I. Initial parameters and main results of the 10:1 mass ratio simulation studied in this work.  $m_{1,2}$  and  $M_{1,2}$  are the bare masses and black-hole masses, respectively. The Bowen-York parameters for the tangential linear momentum  $P$  and the coordinate separation  $D$  are normalized with respect to the total black-hole mass  $M = M_1 + M_2$ . Radiated energy and angular momentum are normalized with respect to their total values for the spacetime. Finally, we give the dimensionless spin and kick parameter of the merged hole.

$m_1$	$m_2$	$M_1$	$M_2$	$M_{\text{ADM}}$	$P/M$	$D/M$	$\frac{E_{\text{rad}}}{M_{\text{ADM}}}$	$\frac{J_{\text{rad}}}{J_{\text{tot}}}$	$j_{\text{fin}}$	$v_{\text{kick}}$
2.4831	0.2303	2.5	0.25	2.7381	0.0415	7.0	$(0.415 \pm 0.017)\%$	$(12.48 \pm 0.62)\%$	$0.259 \pm 0.003$	$66.7 \pm 3.3 \text{ km/s}$

chosen in a certain interval without loss of convergence, which warrants a detailed study in the future. For the present purpose it is sufficient to note that choosing

$$\eta_s = 1.375/M \quad (3)$$

works near both black holes even for  $q = 10$ . We plan to investigate possible benefits of a nonconstant, position dependent  $\eta_s$  (as already suggested in [84,85]) in a future publication.

A computational issue arising for increasing mass ratios is that such simulations typically require more computer time than simulations for comparable masses. The resolution requirement and the time step size is determined by the smaller mass, while the physical time required for one orbit increases with the total mass. We illustrate this by giving rough estimates for the number of computational time steps required for simulating the last three orbits prior to merger. In the equal-mass case  $q = 1$ , reasonable accuracy can be obtained by using a resolution  $h = M/48$  on the finest refinement level corresponding to about 25 000 time steps for the last three orbits. For the present simulation with  $q = 10$ , on the other hand, we obtain the same number of orbits after about 250 000 time steps in the medium resolution case labeled  $N = 68$  below. It is imperative, therefore, to maintain high numerical accuracy over a longer evolution time as we increase  $q$ . A similar increase in computational demands was noted by Lousto and Zlochower [87], who used an additional refinement level for spinning binaries with  $q = 4$  (see their Sec. III).

For these reasons, it is not permissible to infer information on the numerical uncertainties of our simulations by merely extrapolating convergence studies of equal-mass or mildly unequal-mass binaries as obtained, for example, in [4,25]. Instead, we need to study convergence of the present scenario using three resolutions. In the notation of Sec. VI A of [4], our grid setup is given by  $\chi_{\eta_s=1.375}[3 \times N:6 \times 2N:6]$ , where the number of grid points is  $N = 60, 68,$  and  $76$  for the low, medium, and high resolution runs, respectively. In Fig. 1 we show the resulting convergence analysis obtained for the  $\ell = 2, m = 2$  mode of the Newman-Penrose scalar and the radiated energy  $E$  and linear momentum  $P$  extracted at  $r_{\text{ex}} = 36.5 M_{\text{ADM}}$ . For this purpose, we have decomposed the wave signal according to

$$\psi_{22} = A e^{i\phi}, \quad (4)$$

and studied amplitude  $A$  and phase  $\phi$  separately. We observe sixth order convergence for both quantities and the total radiated energy. For the linear momentum  $P = \sqrt{P_x^2 + P_y^2}$ , the convergence is closer to fifth order. We estimate the error due to discretization by comparing the high resolution solution with the Richardson extrapolated result assuming fourth order convergence. We use this more conservative fourth order extrapolation to account for fourth order accurate ingredients in the BAM code. The

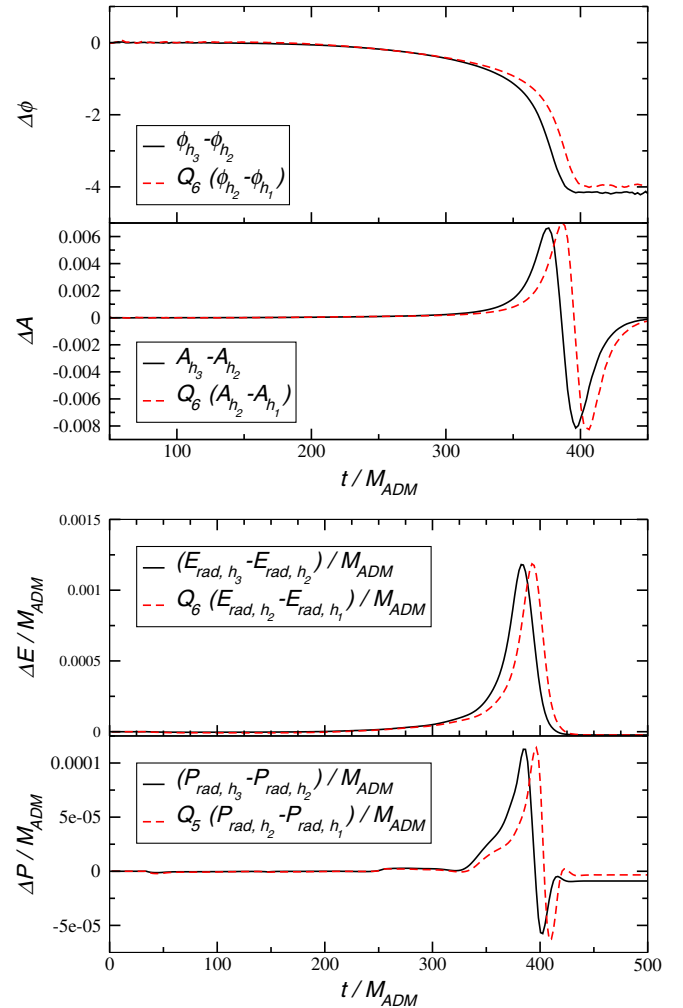


FIG. 1 (color online). Convergence plots for the amplitude  $A$  and phase  $\phi$  of the  $\ell = 2, m = 2$  mode of the Newman-Penrose scalar  $\Psi_4$  (upper panels) as well as the radiated energy  $E$  and linear momentum  $P$  (lower panels). The scaling factors for fifth and sixth order convergence are  $Q_5 = 2.04$  and  $Q_6 = 2.30$ .

uncertainties thus obtained are about 5% for the phase, 1% for the amplitude and radiated energy, and 3% for the recoil and radiated angular momentum. We emphasize that no alignment in phase or time of the wave signal has been applied for this analysis.

We similarly determine the error arising from extracting the waves at finite radius. The extraction radii available for this analysis are  $r_{\text{ex}} = 18.3, 27.4$  and  $36.5 M_{\text{ADM}}$ . For the radiated angular momentum, for example, we obtain at these radii  $J_{\text{rad}} = 12.06, 12.31,$  and  $12.46\%$ , respectively, of  $J_{\text{ini}}$ . These values are well modeled by a function  $a_0 + a_1/r_{\text{ex}}$  which gives us a relative error of about 3.5% for the value extracted at the largest radius  $36.5 M_{\text{ADM}}$ . Similar results are obtained for the other radiated quantities. In the same way, we investigate the phase error of the 22 mode due to the extraction radius. We consider the phase as a function of retarded time  $u = t - r_{\text{ex}}$  and fit for each value

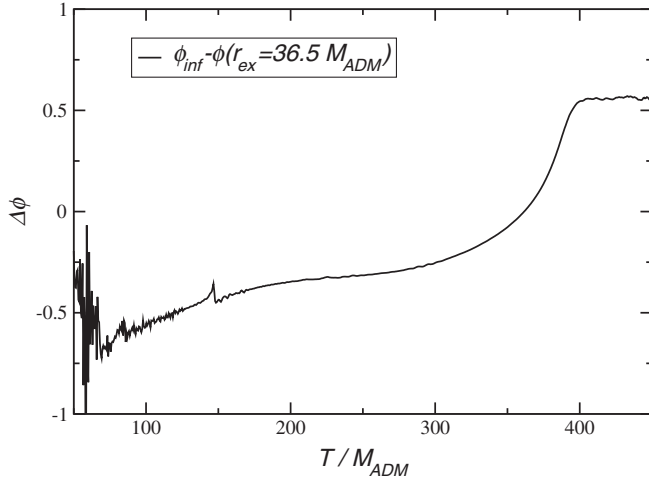


FIG. 2. Difference in phase of the  $\ell = 2$ ,  $m = 2$  mode extrapolated to infinite extraction radius and extracted at  $r_{\text{ex}} = 36.5 M_{\text{ADM}}$ .

of  $u$  the function  $\phi(u, r_{\text{ex}}) = \phi_0(u) + \phi_1(u)/r_{\text{ex}}$ . The difference between the extrapolated phase and the result obtained at  $r_{\text{ex}} = 36.5 M_{\text{ADM}}$  is shown in Fig. 2. The accumulated phase error after coalescence is about  $\Delta\phi = 1.5$  rad, corresponding to a relative error of about 2%. The magnitude of these errors obtained at comparatively small extraction radii seems to suggest that for  $q = 10$  certain near zone effects are reduced compared to  $q = 1$ , although this is to be examined more closely in future work.

We combine the uncertainty estimates due to discretization and extraction radius assuming standard error propagation and adding the squares of the individual errors. We thus obtain error estimates of about 4% for the wave amplitude and radiated energy, 5% for the radiated momenta, and 5.5% for the phase. Note that most of the phase error builds up during the late stages of the inspiral and merger, so that phase uncertainties for performing a comparison with post-Newtonian results will be smaller than the estimate given here. We summarize the results for the radiated energy, momenta, and final spin in Table I, with error bars based on the above analysis.

### III. GRAVITATIONAL WAVE EMISSION

In this section, we study in more detail the gravitational wave emission of the binary. We also discuss the resulting values for radiated energy, final spin, and recoil in the context of general formulas suggested in the literature.

#### A. Comparison with phenomenological formulas

All theoretical modeling of the mass and spin evolution of black holes in the context of their merger history requires a mapping between initial and final black-hole parameters for each individual merger. The generation of such mappings has recently become an industrious area of research, largely because of the breakthroughs in numeri-

cal relativity which make it possible now to simulate black-hole binaries accurately through inspiral, merger, and ringdown. Results are currently available for a relatively small subset of the parameter space only, and have resulted in various efforts to “extrapolate” to wider ranges of the input parameter space using (semi)analytic methods [88–94]. The fitting formulas thus generated have been relatively well tested in the regime of binaries with nearly equal mass or in the test particle limit, but in the regime in between, corresponding to a symmetric mass ratio in the range  $\eta = 0.05, \dots, 0.12$ , accurate data have not as yet been available. Here, we fill this gap and test existing predictions for the case of a nonspinning binary with  $\eta = 0.0826$  or  $q = 10$ .

In Fig. 3, we show the results for the energy radiated in the form of gravitational waves during the last three orbits of the inspiral, the merger, and the ringdown as a function of  $\eta$ . To be precise, we start the integration at a phase  $\Delta\phi = 43.3$  rad in the  $\ell = 2$ ,  $m = 2$  mode prior to the maximum amplitude in that mode. Similar results for mass ratios  $1 \leq q \leq 4$  were presented in [14] and approximated with a polynomial fit in Eq. (3.13) in [25]. Our simulations with  $q = 10$  are in excellent agreement with the amount of gravitational wave energy expected from the polynomial fit. We observe similar agreement with the extrapolated prediction of the peak of the energy flux given in Baker *et al.* [78]. Using their relation (6), we obtain  $\dot{E}_{22,\text{max}} = 3.26 \times 10^{-5}$  to be compared with our numerical result  $\dot{E}_{22,\text{max}} = 3.18 \times 10^{-5}$ . The difference is comfortably within either study’s error estimates.

In Fig. 4, we consider fitting formulas for the final spin of the merged hole taken from Berti *et al.* [25], Rezzolla *et al.* [89], Tichy and Marronetti [91], and Buonanno *et al.* [95] [Eq. (C6) in Baker *et al.* [78]], as well as the effective-one-body predictions by Damour and Nagar [96]. The

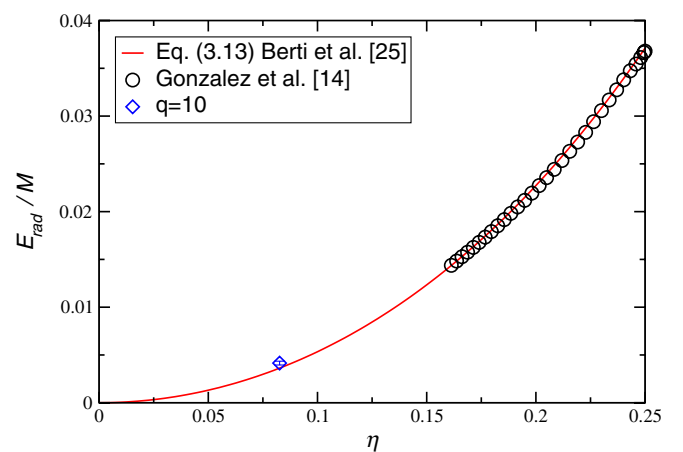


FIG. 3 (color online). Predictions for the energy radiated during the last three orbits (starting at phase 43.3 rad before the maximum in the  $\ell = 2$ ,  $m = 2$  mode), merger, and ringdown are compared with numerical data from [14] as well as new results obtained for the mass ratio  $q = 10:1$ .

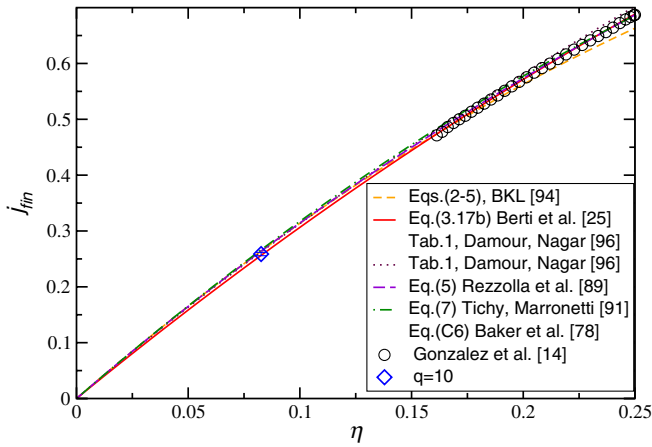


FIG. 4 (color online). Same as Fig. 3 but for the final spin. The curves resulting from Eq. (7) of Tichy and Marronetti and from Eq. (C6) of Baker *et al.* [78,95] would be indistinguishable in this plot and have been represented as the single dash-dotted line. The same applies to the curves resulting from Berti *et al.* [25] and the upper predictions of Damour and Nagar [96], which assume the Kepler law (see their Sec. II).

figure demonstrates that all formulas agree very well with both the results of our previous study [14] in the range  $\eta = 0.16, \dots, 0.25$  and the new value at  $\eta = 0.0826$ . On the other hand, we are not able to discriminate between the different formulas based on our results of nonspinning binaries. The figure also contains the predicted final spin of the model proposed by Buonanno, Kidder, and Lehner (BKL) [94]. The values have been obtained by numerically solving their Eqs. (2–5). Given that they do not fit existing numerical data but model the final spin, their agreement with the numerical results is remarkable. Even for nearly equal masses, the deviations are relatively small, of the order of 5%.

Figure 5 shows a similar analysis for the gravitational recoil using analytic predictions by González *et al.* [14], Baker *et al.* [97], and Schnittman and Buonanno [98]. We

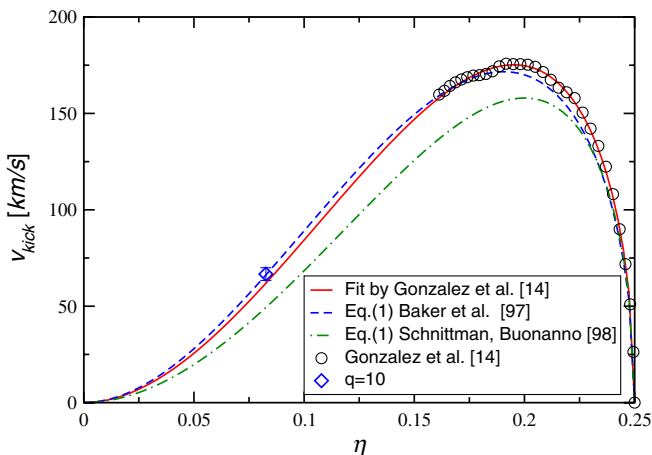


FIG. 5 (color online). Same as Fig. 3 but for the recoil.

thereby additionally test Eq. (2) of Lousto and Zlochower [23], which by construction reduces to the prediction of [14] in the limit of initially nonspinning holes. We further emphasize that Schnittman and Buonanno model the recoil using the effective-one-body method instead of merely fitting available numerical data (cf. BKL for the final spin above). It is natural in this case to expect larger deviations from the numerically obtained values. In analogy to the comparison of the final spin, we observe generally good agreement between predicted values and the numerical results, including  $q = 10$ . This agreement is encouraging, as we believe it highly unlikely that there exist local extrema in either curve in the range  $\eta = 0.05, \dots, 0.15$ , and therefore provides strong support for all formulas in the limit of vanishing initial spin of the holes.

## B. Multipolar structure

Gravitational waves are commonly decomposed into multipoles using spherical harmonics of spin weight  $-2$ . Specifically, the complex Newman-Penrose scalar  $\Psi_4$  extracted at constant radius  $r_{\text{ex}}$  is written as a sum (see e.g. [99])

$$\Psi_4(t, \theta, \phi) = \sum_{\ell, m} \psi_{\ell m}(t) {}_{-2}Y_{\ell m}(\theta, \phi). \quad (5)$$

For illustration, we show in Fig. 6 the real part of the multipole coefficients for  $\ell = m = 2, \dots, 5$ . Most of the earlier studies of black-hole binaries focused on nonspinning, equal-mass systems where  $>98\%$  is radiated in the quadrupole terms  $\ell = 2$ . For more general classes of binaries, however, a significant fraction of the gravitational wave energy is radiated in higher order modes; see e.g. [25]. Simultaneously, the gravitational wave signal predicted for a given orientation of the binary's orbital plane will contain substantial contributions from higher order multipoles and may thus exhibit a pattern much more complex than visible in the quadrupole amplitude  $\psi_{2\pm 2}(t)$ . While this complex multipolar structure places higher demands on the modeling of the gravitational wave sources, it provides us with a large amount of information in the effort to estimate parameters from gravitational wave observations.

A comprehensive study of exploiting such information of higher order multipoles in the context of gravitational wave data analysis is beyond the scope of this paper. In this section we therefore restrict ourselves to a discussion of the multipolar distribution of the gravitational wave energy and merely illustrate the significance of including higher order modes in the waveform for fixed inclination angle of the orbital plane relative to an observer.

The amount of energy contained in different multipoles for the inspiral of binaries with mass ratio  $q = 1, \dots, 4$  has been given in Table IV of [25].

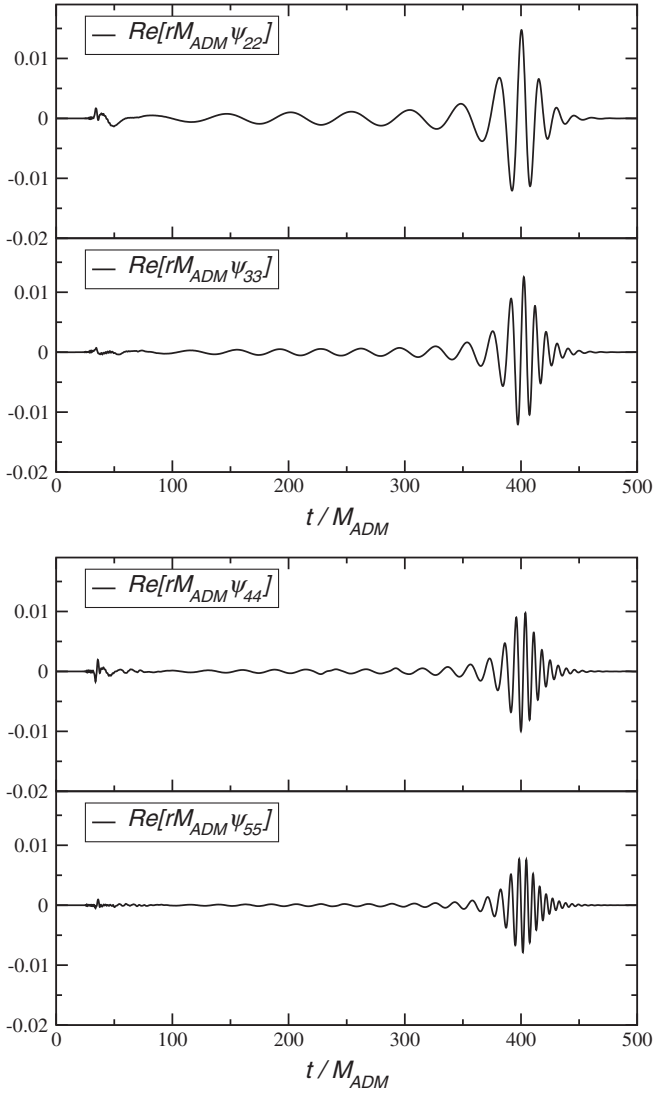


FIG. 6. Multipole coefficients  $r_{\text{ex}} M_{\text{ADM}} \psi_{\ell m}$  for  $\ell = m = 2, \dots, 5$  extracted at  $36.5 M_{\text{ADM}}$ .

We graphically display the energy contained in the multipoles in Fig. 7. Here, the upper panel displays the energy contained in the multipoles corresponding to a particular value of  $\ell$ , whereas the symbols in the lower panel show the fractional energy contained in all modes up to  $\ell \leq \ell_{\text{max}}$ . We discard the first  $50 M_{\text{ADM}}$  of the waveform, which is dominated by spurious radiation inherent to the initial data. This corresponds to the radiated energy starting at phase 43.3 rad prior to the maximum in the  $\ell = 2, m = 2$  mode. The resulting energy is well approximated by quadratic polynomials. Specifically, we obtain the following fits for the numerical data in the range  $1 \leq q \leq 10$  corresponding to  $0.25 \geq \eta \geq 0.0826$ :

$$E_{\ell=2}/E_{\text{rad}} = 68.0 + 80.4\eta + 159.2\eta^2, \quad (6)$$

$$E_{\ell \leq 3}/E_{\text{rad}} = 84.6 + 108.8\eta - 212.7\eta^2, \quad (7)$$

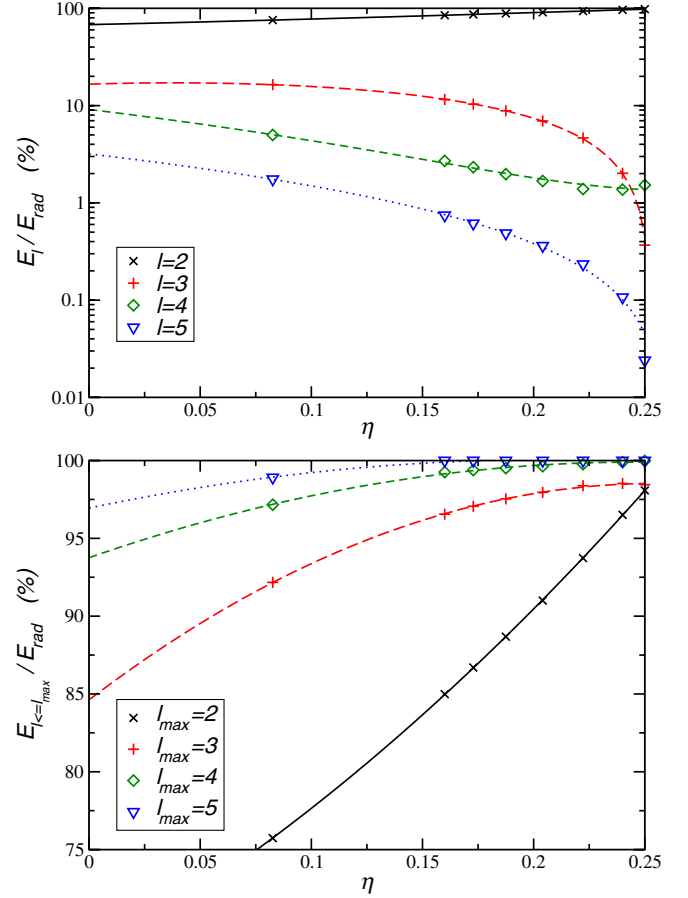


FIG. 7 (color online). The energy contained in the individual multipoles  $\ell = \text{const}$  (upper panel) as well as the energy radiated in all modes up to a given  $\ell_{\text{max}}$  (lower panel) as a function of the dimensionless mass parameter  $\eta$ .

$$E_{\ell \leq 4}/E_{\text{rad}} = 93.8 + 49.9\eta - 101.3\eta^2, \quad (8)$$

$$E_{\ell \leq 5}/E_{\text{rad}} = 96.9 + 30.0\eta - 72.1\eta^2. \quad (9)$$

The trend for higher order multipoles to carry a larger fraction of the total radiated energy  $E_{\text{rad}}$  is clearly maintained for  $q = 10$ . Close inspection of  $E_{\ell=3}$  reveals a local maximum near  $\eta = 0.04$ . We believe this to be an artifact of the limited accuracy of the data and the polynomial fits.

The significance of higher multipoles also reveals itself in the gravitational wave signal observed at fixed values for the inclination angle  $\theta$  of the orbital plane of the binary. The combination of all multipoles in the signal  $\Psi_4$  shows a much more complex structure than the quadrupole on its own. We illustrate this in Fig. 8 where we plot the real and imaginary parts of  $\Psi_4$  at  $r_{\text{ex}} = 36.5 M_{\text{ADM}}$  and  $\theta = 45.5^\circ$ . The inclination angle has been chosen somewhat arbitrarily, but we get the same general result for other choices of  $\theta$ . The pattern resulting from the inclusion of the octupole and higher order modes in the bottom panels of Fig. 8 shows a nonmonotonic increase in the local maxima of the wave signal during inspiral which is reminiscent of the

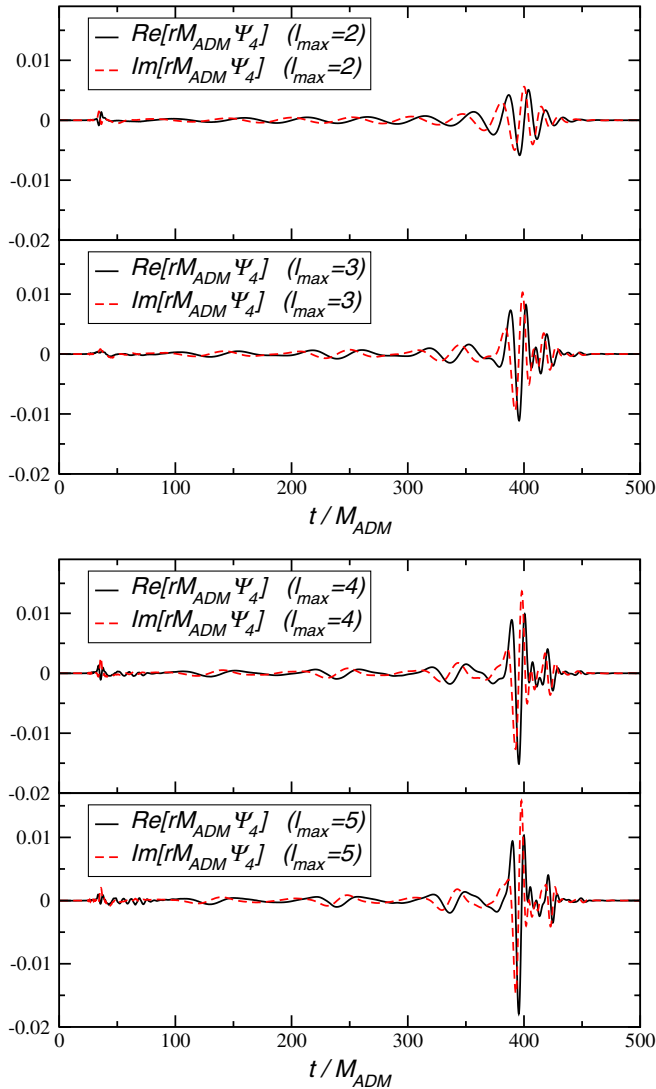


FIG. 8 (color online). The Newman-Penrose scalar  $\Psi_4$  obtained at an inclination of the orbital plane of  $\theta = 45.5^\circ$  including multipoles up to and including  $\ell_{\max} = 2, 3, 4$ , and 5 (from top to bottom).

pure quadrupole signal in eccentric inspirals (cf. the “MayaKranc e02” entry in Fig. 1 of Ref. [100]). In contrast, there is little evidence of eccentricity if we consider the individual modes of our simulation in Fig. 6. As a further impact of the higher order multipoles, we note the significant increase in the amplitude between the top and bottom panels of Fig. 8.

These observations qualitatively illustrate the importance of including higher order multipoles in gravitational wave data analysis, as has been pointed out quantitatively in the literature [25,78,101–106].<sup>1</sup> In future work, we plan

<sup>1</sup>Higher order harmonics as discussed in some of these references are not strictly equivalent to higher order multipoles but often imply the inclusion of additional multipoles.

to investigate this issue more systematically using our numerical data in the context of matched filtering.

#### IV. CONCLUSIONS

In this work, we have pushed the mass ratio in numerical simulations of inspiralling black-hole binaries significantly beyond what has previously been published. Our simulations have been demonstrated to be convergent consistently with the discretization properties of the numerical code. We have resolved an issue specific to larger mass ratios by choosing a specific value of the shift damping parameter. The overall errors in wave amplitude and phase as well as radiated energy and momenta are about 5%. We have thus been able to validate existing fitting formulas for the amount of energy and linear momentum as well as the final spin of the merging hole in a range of the mass ratio previously unexplored. Within the error bars, we find our numerical results to be in agreement with phenomenological formulas. These are of high importance in the modeling of astrophysical phenomena, such as the growth of supermassive black holes. At least in the case of nonspinning holes, we conjecture that the fitting formulas can be used over the entire range of the dimensionless mass ratio parameter  $\eta$ .

Extending previous work [25], we have further demonstrated that the percentage of gravitational wave energy radiated in higher order multipoles increases significantly as the mass ratio deviates from the equal-mass limit  $\eta = 0.25$  or  $q = 1$ . Quadratic fitting of our numerical data indicates that about 32% of the total radiated energy will be contained in  $\ell > 2$  as the EMR limit is approached. For the  $q = 10$  case at hand, we find about 25% of the energy to be contained in modes higher than the quadrupole. This distribution of the energy also manifests itself in the shape of the gravitational waveform as measured for a fixed inclination of the binary orbit relative to the observer. The case  $\theta \approx 45^\circ$  exhibits a significant change in the wave signal as we include higher order multipoles. While we only display results for one value of  $\theta$ , we find this behavior to be similar for arbitrary alternative inclinations.

It will be important to extend the current study to spinning binaries in the future. This will allow us to address various important questions in astrophysics and gravitational wave physics. For example, there remain uncertainties about the magnitude of the recoil effect for spinning binaries of unequal mass [15,87,97]. Also, it will be important to compare fitting formulas for final spin and recoil with numerical results for initially spinning black holes.

The use of numerical waveforms in gravitational wave data analysis further requires careful comparisons with post-Newtonian predictions and the combination of numerical with post-Newtonian waveforms (e.g. [105,107–114]). In future work, we plan to perform such comparisons, including various post-Newtonian techniques. We also believe that the current simulations facilitate approxi-

mate comparisons with perturbative calculations of EMR binaries. Finally, an intriguing question concerns the properties of black-hole collisions or scattering experiments involving unequal-mass binaries traveling close to the speed of light. Studies have so far been restricted to collisions of nonspinning equal-mass binaries [115,116] and predict that as much as  $\sim 14\%$  of the total energy of the system can be radiated in head-on collisions and even larger quantities for nonzero impact parameters.

In summary, accurate simulations of black-hole binaries with mass ratio  $q = 10$  are not only possible using current numerical techniques (if somewhat expensive), but also reveal a richness in structure beyond what has been observed in the nearly equal-mass case. We consider our simulations of the nonspinning case to be the starting point of more exhaustive studies involving spins and/or eccentricity, which will be of significant value for current efforts to observe gravitational waves and improve our under-

standing of astrophysical questions involving the merger of black-hole binaries.

## ACKNOWLEDGMENTS

It is a pleasure to thank Emanuele Berti, Vitor Cardoso, Mark Hannam, Sascha Husa, and Doreen Müller for discussions. This work was supported in part by DFG Grant No. SFB/Transregio 7 “Gravitational Wave Astronomy,” the DLR (Deutsches Zentrum für Luft und Raumfahrt), by grants from the Sherman Fairchild Foundation to Caltech, by NSF Grant No. PHY-0601459, No. PHY-0652995 and No. PHY-090003, by grant CIC 4.23 to Universidad Michoacana, PROMEP UMICH-PTC-210 and UMICH-CA-22 from SEP México and CONACyT Grant No. 79601. Computations were performed on the HLRB2 at LRZ Munich. We acknowledge support from the ILIAS Sixth Framework programme.

- 
- [1] F. Pretorius, *Phys. Rev. Lett.* **95**, 121101 (2005).
  - [2] J. G. Baker, J. Centrella, D.-I. Choi, M. Koppitz, and J. van Meter, *Phys. Rev. Lett.* **96**, 111102 (2006).
  - [3] M. Campanelli, C. O. Lousto, P. Marronetti, and Y. Zlochower, *Phys. Rev. Lett.* **96**, 111101 (2006).
  - [4] B. Brügmann, J. A. González, M. D. Hannam, S. Husa, U. Sperhake, and W. Tichy, *Phys. Rev. D* **77**, 024027 (2008).
  - [5] F. Pretorius, *Classical Quantum Gravity* **23**, S529 (2006).
  - [6] J. G. Baker, J. Centrella, D.-I. Choi, M. Koppitz, and J. van Meter, *Phys. Rev. D* **73**, 104002 (2006).
  - [7] M. Campanelli, C. O. Lousto, and Y. Zlochower, *Phys. Rev. D* **73**, 061501(R) (2006).
  - [8] F. Herrmann, I. Hinder, D. Shoemaker, and P. Laguna, *Classical Quantum Gravity* **24**, S33 (2007).
  - [9] U. Sperhake, *Phys. Rev. D* **76**, 104015 (2007).
  - [10] D. Pollney *et al.*, *Phys. Rev. D* **76**, 124002 (2007).
  - [11] Z. B. Etienne, J. A. Faber, Y. T. Liu, S. L. Shapiro, and T. W. Baumgarte, *Phys. Rev. D* **76**, 101503(R) (2007).
  - [12] M. A. Scheel, M. Boyle, T. Chu, L. E. Kidder, K. D. Matthews, and H. P. Pfeiffer, *Phys. Rev. D* **79**, 024003 (2009).
  - [13] F. Pretorius, arXiv:0710.1338.
  - [14] J. A. González, U. Sperhake, B. Brügmann, M. D. Hannam, and S. Husa, *Phys. Rev. Lett.* **98**, 091101 (2007).
  - [15] M. Campanelli, C. O. Lousto, Y. Zlochower, and D. Merritt, *Astrophys. J.* **659**, L5 (2007).
  - [16] J. A. González, M. D. Hannam, U. Sperhake, B. Brügmann, and S. Husa, *Phys. Rev. Lett.* **98**, 231101 (2007).
  - [17] M. Campanelli, C. O. Lousto, Y. Zlochower, and D. Merritt, *Phys. Rev. Lett.* **98**, 231102 (2007).
  - [18] F. Healy, J. Herrmann, I. Hinder, D. Shoemaker, P. Laguna, and R. A. Matzner, *Phys. Rev. Lett.* **102**, 041101 (2009).
  - [19] J. G. Baker, J. Centrella, D.-I. Choi, M. Koppitz, J. van Meter, and M. C. Miller, *Astrophys. J.* **653**, L93 (2006).
  - [20] F. Herrmann, I. Hinder, D. Shoemaker, P. Laguna, and R. A. Matzner, *Astrophys. J.* **661**, 430 (2007).
  - [21] M. Koppitz, D. Pollney, C. Reisswig, L. Rezzolla, J. Thornburg, P. Diener, and E. Schnetter, *Phys. Rev. Lett.* **99**, 041102 (2007).
  - [22] B. Brügmann, J. A. González, M. D. Hannam, S. Husa, and U. Sperhake, *Phys. Rev. D* **77**, 124047 (2008).
  - [23] C. O. Lousto and Y. Zlochower, *Phys. Rev. D* **77**, 044028 (2008).
  - [24] M. Campanelli, C. O. Lousto, Y. Zlochower, B. Krishnan, and D. Merritt, *Phys. Rev. D* **75**, 064030 (2007).
  - [25] E. Berti, V. Cardoso, J. A. González, U. Sperhake, M. D. Hannam, S. Husa, and B. Brügmann, *Phys. Rev. D* **76**, 064034 (2007).
  - [26] T. Baumgarte, P. Brady, J. D. E. Creighton, L. Lehner, F. Pretorius, and R. De Voe, *Phys. Rev. D* **77**, 084009 (2008).
  - [27] A. Buonanno, G. B. Cook, and F. Pretorius, *Phys. Rev. D* **75**, 124018 (2007).
  - [28] P. Ajith *et al.*, *Classical Quantum Gravity* **24**, S689 (2007).
  - [29] P. Ajith *et al.*, *Phys. Rev. D* **77**, 104017 (2008).
  - [30] B. Vaishnav, I. Hinder, F. Herrmann, and D. Shoemaker, *Phys. Rev. D* **76**, 084020 (2007).
  - [31] M. Shibata and K. Uryu, *Classical Quantum Gravity* **24**, S125 (2007).
  - [32] M. Anderson, E. W. Hirschmann, L. Lehner, S. L. Liebling, P. M. Motl, D. Neilsen, C. Palenzuela, and J. E. Tohline, *Phys. Rev. D* **77**, 024006 (2008).
  - [33] Z. B. Etienne, J. A. Faber, Y. T. Liu, S. L. Shapiro, K. Taniguchi, and T. W. Baumgarte, *Phys. Rev. D* **77**, 084002 (2008).
  - [34] L. Baiotti, B. Giacomazzo, and L. Rezzolla, *Phys. Rev. D* **78**, 084033 (2008).
  - [35] M. D. Duez, F. Foucart, L. E. Kidder, H. P. Pfeiffer, M. A. Scheel, and S. A. Teukolsky, *Phys. Rev. D* **78**, 104015 (2009).



- (2008).
- [36] B. Abbott *et al.*, arXiv:0711.3041.
- [37] F. Beauville *et al.*, *Classical Quantum Gravity* **25**, 045002 (2008).
- [38] H. Lueck *et al.*, *Classical Quantum Gravity* **23**, S71 (2006).
- [39] D. Tatsumi *et al.*, *Classical Quantum Gravity* **24**, S399 (2007).
- [40] A. Sesana, M. Volonteri, and F. Haardt, *Mon. Not. R. Astron. Soc.* **377**, 1711 (2007).
- [41] L. A. Gergely and P. L. Biermann, arXiv:0704.1968.
- [42] A. Buonanno and T. Damour, *Phys. Rev. D* **59**, 084006 (1999).
- [43] T. Damour, B. R. Iyer, and B. S. Sathyaprakash, *Phys. Rev. D* **57**, 885 (1998).
- [44] T. Damour, B. R. Iyer, and B. S. Sathyaprakash, *Phys. Rev. D* **63**, 044023 (2001).
- [45] K. G. Arun, L. Blanchet, B. R. Iyer, and M. S. S. Qusailah, *Classical Quantum Gravity* **21**, 3771 (2004).
- [46] L. Blanchet, *Living Rev. Relativity* **9**, 4 (2006), <http://www.livingreviews.org/Articles/lrr-2006-4/download/index.html>.
- [47] Y. Mino, M. Sasaki, and T. Tanaka, *Prog. Theor. Phys. Suppl.* **128**, 373 (1997).
- [48] E. Poisson, *Living Rev. Relativity* **7**, 6 (2004), <http://relativity.livingreviews.org/Articles/lrr-2004-6/download/index.html>.
- [49] S. A. Hughes, *AIP Conf. Proc.* **873**, 233 (2006).
- [50] S. Detweiler, *Phys. Rev. D* **77**, 124026 (2008).
- [51] N. Yunes and E. Berti, *Phys. Rev. D* **77**, 124006 (2008).
- [52] T. Damour and A. Nagar, *Phys. Rev. D* **76**, 064028 (2007).
- [53] T. Hinderer and E. E. Flanagan, *Phys. Rev. D* **78**, 064028 (2008).
- [54] J. E. McClintock, R. Shafee, R. Narayan, R. A. Remillard, S. W. Davis, and L.-X. Li, *Astrophys. J.* **652**, 518 (2006).
- [55] S. W. Davis and I. Hubeny, arXiv:astro-ph/0602499.
- [56] M. Middleton, C. Done, M. Gierlinński, and S. W. Davis, arXiv:astro-ph/0601540.
- [57] R. Shafee, J. E. McClintock, R. Narayan, S. W. Davis, L. Li, and R. A. Remillard, *Astrophys. J.* **636**, L113 (2006).
- [58] J. Wilms, C. S. Reynolds, M. C. Begelman, J. Reeves, S. Molendi, R. Staubert, and E. Kendziorra, *Mon. Not. R. Astron. Soc.* **328**, L27 (2001).
- [59] M. Elvis, G. Risaliti, and G. Zamorani, *Astrophys. J.* **565**, L75 (2002).
- [60] J.-M. Wang, Y.-M. Chen, L. C. Ho, and R. J. McLure, *Astrophys. J.* **642**, L111 (2006).
- [61] C. F. Gammie, S. L. Shapiro, and J. C. McKinney, *Astrophys. J.* **602**, 312 (2004).
- [62] S. L. Shapiro, *Astrophys. J.* **620**, 59 (2005).
- [63] E. Berti and M. Volonteri, *Astrophys. J.* **684**, 822 (2008).
- [64] S. A. Hughes and R. D. Blandford, *Astrophys. J.* **585**, L101 (2003).
- [65] M. Voonteri, P. Madau, E. Quataert, and M. Rees, *Astrophys. J.* **620**, 69 (2005).
- [66] A. R. King and J. E. Pringle, *Mon. Not. R. Astron. Soc.* **373**, L90 (2006).
- [67] A. R. King, J. E. Pringle, and J. A. Hofmann, *Mon. Not. R. Astron. Soc.* **385**, 1621 (2008).
- [68] I. H. Redmount and M. J. Rees, *Comments Astrophys.* **14**, 165 (1989).
- [69] M. Boylan-Kolchin, C.-P. Ma, and E. Quataert, *Astrophys. J.* **613**, L37 (2004).
- [70] Z. Haiman, *Astrophys. J.* **613**, 36 (2004).
- [71] P. Madau and E. Quataert, *Astrophys. J.* **606**, L17 (2004).
- [72] D. Merritt, M. Milosavljević, M. Favata, S. Hughes, and D. Holz, *Astrophys. J.* **607**, L9 (2004).
- [73] N. I. Libeskind, S. Cole, C. S. Frenk, and J. C. Helly, *Mon. Not. R. Astron. Soc.* **368**, 1381 (2006).
- [74] L. Blecha and A. Loeb, arXiv:0805.1420.
- [75] S. Komossa, H. Zhou, and H. Lu, *Astrophys. J.* **678**, L81 (2008).
- [76] S. Komossa and D. Merritt, *Astrophys. J.* **683**, L21 (2008).
- [77] K. Menou, Z. Haiman, and B. Kocsis, *New Astron. Rev.* **51**, 884 (2008).
- [78] J. G. Baker, W. D. Boggs, J. Centrella, B. J. Kelly, S. T. McWilliams, and J. R. van Meter, *Phys. Rev. D* **78**, 044046 (2008).
- [79] B. Brügmann, W. Tichy, and N. Jansen, *Phys. Rev. Lett.* **92**, 211101 (2004).
- [80] S. Husa, J. A. González, M. D. Hannam, B. Brügmann, and U. Sperhake, *Classical Quantum Gravity* **25**, 105006 (2008).
- [81] M. Ansorg, B. Brügmann, and W. Tichy, *Phys. Rev. D* **70**, 064011 (2004).
- [82] A. Nerozzi and O. Elbracht, arXiv:0811.1600.
- [83] U. Sperhake, E. Berti, V. Cardoso, J. A. González, B. Brügmann, and M. Ansorg, *Phys. Rev. D* **78**, 064069 (2008).
- [84] M. Alcubierre, B. Brügmann, D. Pollney, E. Seidel, and R. Takahashi, *Phys. Rev. D* **64**, 061501(R) (2001).
- [85] M. Alcubierre, B. Brügmann, P. Diener, M. Koppitz, D. Pollney, E. Seidel, and R. Takahashi, *Phys. Rev. D* **67**, 084023 (2003).
- [86] J. R. van Meter, J. G. Baker, M. Koppitz, and D.-I. Choi, *Phys. Rev. D* **73**, 124011 (2006).
- [87] C. O. Lousto and Y. Zlochower, *Phys. Rev. D* **79**, 064018 (2009).
- [88] L. Rezzolla, E. N. Dorband, C. Reisswig, P. Diener, D. Pollney, E. Schnetter, and B. Szilagyi, *Astrophys. J.* **679**, 1422 (2008).
- [89] L. Rezzolla, P. Diener, E. N. Dorband, D. Pollney, C. Reisswig, and E. Schnetter, *Astrophys. J.* **674**, L29 (2008).
- [90] L. Rezzolla, E. Barausse, E. N. Dorband, D. Pollney, C. Reisswig, J. Seiler, and S. Husa, *Phys. Rev. D* **78**, 044002 (2008).
- [91] W. Tichy and P. Marronetti, *Phys. Rev. D* **78**, 081501 (2008).
- [92] L. Boyle, M. Kesden, and S. Nissanke, *Phys. Rev. Lett.* **100**, 151101 (2008).
- [93] L. Boyle and M. Kesden, *Phys. Rev. D* **78**, 024017 (2008).
- [94] A. Buonanno, L. E. Kidder, and L. Lehner, *Phys. Rev. D* **77**, 026004 (2008).
- [95] A. Buonanno, Y. Pan, J. G. Baker, J. Centrella, B. J. Kelly, S. T. McWilliams, and J. R. van Meter, *Phys. Rev. D* **76**, 104049 (2007).
- [96] T. Damour and A. Nagar, *Phys. Rev. D* **76**, 044003 (2007).
- [97] J. G. Baker *et al.*, *Astrophys. J.* **682**, L29 (2008).
- [98] J. D. Schnittman and A. Buonanno, arXiv:astro-ph/0702641.
- [99] K. S. Thorne, *Rev. Mod. Phys.* **52**, 299 (1980).
- [100] B. Aylott *et al.*, arXiv:0901.4399.

- [101] C. Van Den Broeck and A.S. Sengupta, *Classical Quantum Gravity* **24**, 155 (2007).
- [102] C. Van Den Broeck, *Classical Quantum Gravity* **23**, L51 (2006).
- [103] K. G. Arun, B. R. Iyer, B. S. Sathyaprakash, and S. Sinha, *Phys. Rev. D* **75**, 124002 (2007).
- [104] K. G. Arun, B. R. Iyer, B. S. Sathyaprakash, S. Sinha, and C. Van Den Broeck, *Phys. Rev. D* **76**, 104016 (2007).
- [105] Y. Pan, A. Buonanno, J. G. Baker, J. Centrella, B. J. Kelly, S. T. McWilliams, F. Pretorius, and J. R. van Meter, *Phys. Rev. D* **77**, 024014 (2008).
- [106] E. K. Porter and N. J. Cornish, *Phys. Rev. D* **78**, 064005 (2008).
- [107] M. D. Hannam, S. Husa, J. A. González, U. Sperhake, and B. Brügmann, *Phys. Rev. D* **77**, 044020 (2008).
- [108] M. Boyle, D. A. Brown, L. E. Kidder, A. H. Mroué, H. P. Pfeiffer, M. A. Scheel, G. B. Cook, and S. A. Teukolsky, *Phys. Rev. D* **76**, 124038 (2007).
- [109] M. Campanelli, C. O. Lousto, H. Nakano, and Y. Zlochower, *Phys. Rev. D* **79**, 084010 (2009).
- [110] A. Gopakumar, M. D. Hannam, S. Husa, and B. Brügmann, *Phys. Rev. D* **78**, 064026 (2008).
- [111] T. Damour, A. Nagar, M. D. Hannam, S. Husa, and B. Brügmann, *Phys. Rev. D* **78**, 044039 (2008).
- [112] J. G. Baker, J. R. van Meter, S. T. McWilliams, J. Centrella, and B. J. Kelly, *Phys. Rev. Lett.* **99**, 181101 (2007).
- [113] I. Hinder, F. Herrmann, P. Laguna, and D. Shoemaker, arXiv:0806.1037.
- [114] M. Boyle, A. Buonanno, L. E. Kidder, A. H. Mroue, Y. Pan, H. P. Pfeiffer, and M. A. Scheel, *Phys. Rev. D* **78**, 104020 (2008).
- [115] U. Sperhake, V. Cardoso, F. Pretorius, E. Berti, and J. A. Gonzalez, *Phys. Rev. Lett.* **101**, 161101 (2008).
- [116] M. Shibata, H. Okawa, and T. Yamamoto, *Phys. Rev. D* **78**, 101501(R) (2008).